Measurement accuracy analysis of the free carrier absorption determination of the electronic transport properties of silicon wafers*

Zhang Xi-Ren(张希仁)†, Gao Chun-Ming(高椿明),
Zhou Ying(周 鹰), and Wang Zhan-Ping(王占平)

School of Optoelectronic Information, University of Electronic Science and Technology of China, Chengdu 610054, *China*

(Received 14 September 2010; revised manuscript received 14 January 2011)

By introducing the random and systematic errors in simulated data computed from conventional frequency-scan and laterally resolved modulated free carrier absorption theory models, we investigate the relative determination sensitivities of three electronic transport properties, namely, carrier lifetime, carrier diffusivity and front surface recombination velocity of silicon wafers determined by frequency-scan and laterally resolved techniques. The phase and amplitude data with random errors as functions of the modulation frequency at zero pump-probe-beam separation or of the two-beam separation at four different modulation frequencies are simultaneously fitted to an appreciated carrier diffusion model to extract three transport parameters. The statistical results and fitted accuracies of the transport parameter determined by both techniques are theoretically analysed. Corresponding experimental results are carried out to compare to the simulated results. The simulated and experimental results show that the determination of the transport properties of silicon wafers by the laterally resolved technique are more accurate, as compared with that by the frequency-scan technique.

Keywords: laterally resolved modulated free-carrier absorption, frequency scans, electronic transport properties, accuracy

PACS: 81.70.Fy, 72.02.Jv, 72.10.–d **DOI:** 10.1088/1674-1056/20/6/068105

1. Introduction

In order to build a silicon-based microelectronic device that provides optimal performance, it is necessary to characterize the electronic transport properties of semiconductors (i.e., the carrier lifetime τ, the carrier diffusivity D and the front surface recombination velocity s_1 (FSRV)) before, during and after processing. Until now, numerous nondestructive optical techniques based on modulated photoexcitation, such as modulated free carrier absorption (MFCA),[1−4] photo-carrier radiometry (PCR),[5−8] photo-modulated thermoreflectance (PMR),[9−11] and infrared photothermal radiometry (PTR),[12−14] have been developed and implemented into the transport property characterization of semiconductors. In PMR and PTR both thermal and free-carrier waves contributing to the signal have resulted in signal interpretational and computational difficulties due to the large number of variables involved and thus given rise to the question of uniqueness of the measured set of transport parameters. The major advantage of MFCA and PCR over PMR and PTR has been found to be that there is only the free-carrier contribution to the signals and thus the transport properties of semiconductors can be determined more accurately. However, recent investigations[8,15] have demonstrated that the determination accuracies of carrier lifetime and FSRV can be unacceptable unless the carrier diffusivity D is known in advance with high precision. Unfortunately, it has been indicated from investigations by Rodriguez *et al.*[16] that the carrier diffusivity values of most wafers depend on the injection level and process parameters, and, as a result, the carrier diffusivities vary widely. This carrier diffusivity uncertainty causes considerable deviations of both fitted τ and s_1 from the real values of measured wafers.

Until recently, a laterally resolved MFCA technique (LR-MFCA) was proposed by Zhang *et al.*,[17] which has a number of potential advantages over conventional MFCA and other existing methods, and it has been employed to characterize the electronic transport properties of semiconductors. It was justified in a previous paper[18,19] that unlike the dependences of conventional frequency-scan MFCA (FS-MFCA) and

*Project supported by the Fundamental Research Funds for the Central Universities of China (Grant No. ZYGX2009J051).
†Corresponding author. E-mail: xiren3208@163.com
© 2011 Chinese Physical Society and IOP Publishing Ltd

PCR signals on the modulation frequency, the LR-MFCA signals are dependent on the pump-probe-beam separation and highly sensitive to the lifetime and FSRV, especially to the diffusivity and thus D, τ and s_1 can be simultaneously obtained with high precision. However, until now, no quantitative analysis has yet been done regarding the relative determination accuracies of the transport properties by the FS- and LR-MFCAs.

In this article, computer simulation is performed to analyse the relative measurement accuracies and to estimate the uncertainty of the fitted transport parameters by the FS- and LR-MFCAs via a multi-parameter fit procedure. First, sets of amplitude and phase data as functions of modulation frequency at zero probe-pump offset for FS-MFCA, and of probe-pump offset at four different modulation frequencies for LR-MFCA are created, respectively, by introducing both random and systematic errors into the amplitude and phase behaviour calculated with a rigorous three-dimensional carrier diffusion model. Then, these data sets with errors are multiparameter fitted with the same carrier diffusion model to extract the lifetime, diffusivity and FSRV by minimizing the mean square variance for the FS- and LR-MFCAs. This fitted procedure is repeated 30 times with data sets with different errors. The statistical results of these simulations are then analysed and compared to the input transport parameter values. Additionally, the comparison between the statistical results obtained by these two methods is done and the relative accuracies of fitted results are estimated. Finally, corresponding experimental results are presented and compared to the simulated results.

2. Theoretical model

In the MFCA technique, an intensity-modulated beam (with photo-energy greater than the energy gap of wafer) used as pump beam periodically generates an excess carrier within the sample. Subsequently, there is an excess carrier population in the sample by carrier diffusion and recombination at the surface and in the bulk of the sample. This process is monitored by another probe beam (with a photo-energy below the energy gap of wafer) transmitting to the sample. The excess carrier absorption in the probe beam (free-carrier absorption) induces the fractional modulation of the probe beam intensity, which is proportional to the number of free carriers that the probe beam encounters along its path within the sample. Then the MFCA signal can be expressed as follows:[18]

$$\frac{\Delta I(\omega;r)}{I} = -\text{const} \times \int_0^\infty F(k,\omega)\mathrm{J}_0(kr)k\mathrm{d}k, \quad (1)$$

where

$$\begin{aligned} F(k,\omega) = {} & \frac{\mathrm{e}^{-k^2W^2/4}}{(\alpha^2-b_n^2)}\left[\left(\frac{G_2g_1-g_2G_1\mathrm{e}^{-(b_n+\alpha)L}}{G_2-G_1\mathrm{e}^{-2b_nL}}\right.\right. \\ & \left.\left.+\frac{g_1\mathrm{e}^{-b_nL}-g_2\mathrm{e}^{-\alpha L}}{G_2-G_1\mathrm{e}^{-2b_nL}}\right)\frac{(1-\mathrm{e}^{-b_nL})}{b_n} \right. \\ & \left. -\frac{1-\mathrm{e}^{-\alpha L}}{\alpha}\right], \\ b_n^2 = {} & k^2+\sigma_n^2, \quad \sigma_n^2 = \frac{1+\mathrm{j}\omega\tau}{D\tau}, \\ g_1 = {} & \frac{D\alpha+s_1}{Db_n+s_1}, \quad g_2 = \frac{D\alpha+s_2}{Db_n-s_2}, \\ G_1 = {} & \frac{Db_n-s_1}{Db_n+s_1}, \quad G_2 = \frac{Db_n+s_2}{Db_n-s_2}. \end{aligned}$$

Here, α, L, and s_2 are the absorption coefficient, thickness and rear surface recombination velocity (RSRV) of the semiconductor wafer, respectively. I and ΔI are the un-modulated and modulated portions of the intensity of the transmitted probe beam; $\omega = 2\pi f$ with f the modulation frequency of the pump beam intensity and r is the pump–probe–beam separation. W is the effective radius of the pump beam.

It is found from Eq. (1) that the entire MFCA data contain information of the transport properties of the specimen, the size of both the pump and the probe beams and their separation, as well as the modulation frequency of the pump beam. Therefore, the three transport parameters, τ, D, and s_1, of the semiconductor wafer can be extracted by measuring the dependence of the MFCA signal on the modulation frequency (FS-MFCA)[2] or on the pump–probe–beam separation (LR-MFCA)[17,18] via multi-parameter fitting.

In order to determine the transport parameters of the silicon wafers by fitting the experimental data of LR- and FS-MFCA amplitude and phase to the rigorous theoretical model [Eq. (1)], the mean square variances for FS- and LR-MFCAs must be minimized. Here, the mean square variance for LR-MFCA is defined in Ref. [18] and that for FS-MFCA defined in Ref. [19].

3. Simulation

In this section, computer simulations are performed to show the relative determination accuracies of the carrier lifetime, the carrier diffusivity, and FSRV of silicon wafers by FS- or LR-MFCA methods when experimental errors are introduced into the

simulations. The experimental parameters and their respective errors are set according to the experimental details.[17,18] In our simulations, RSRV is fixed to 10^4 cm/s, since RSRV has little effect on the MFCA signal and is an insignificant transport parameter of silicon wafers used in micro-electronic devices.[8]

In the MFCA experiment, the amplitude and phase measurement errors depend on the time constant of the lock-in amplifier. In the FS-MFCA simulations we assume ±2% normally distributed amplitude and phase errors. However, in LR-MFCA we assume ±4% normally distributed amplitude and phase errors, which are higher than those in FS-MFCA. This is due to the fact that with increasing two-beam separation, the decrease in the signal results in the decrease of the signal-to-noise ratio and then the increase of the measurement errors. Since a mechanical motorized stage is used to move the turning mirror and to focus the lens assembly in LR-MFCA, there may be a small misalignment in pump–probe–beam separation. Therefore, we assume a ±3-μm offset in a two-beam separation. In the FS- and LR-MFCA experiments, both exciting and probe beams are focused onto the sample surface. The effective size of the exciting spot is the convolution of the pump and probe spots. A Gaussian spot with a focusing radius of 25 μm is assumed in our simulations. In the FS-MFCA method, the lifetime and FSRV can be determined accurately only when the effective radius of pump beam is known previously with high precision. In practice, it is difficult to accurately measure the radii of the pump and probe beams in the experiments. Therefore, due to possible misalignment, we assume a maximum ±3-μm error in the spot radius, i.e., the radius lies randomly between 22 μm and 28 μm in FS-MFCA. On the other hand, since the signal of the LR-MFCA is particularly sensitive to the radius of exciting beam, the radius set as a free parameter can be extracted with a multi-parameter fit procedure. During the measurement period at each frequency, a small frequency shift (0.2%) is also assumed for both FS- and LR-MFCA. A summary of the assumed experimental errors is given in Table 1.

Table 1. Assumed experimental errors in the simulated FS- and LR-MFCA amplitude and phase data.

	Parameter	Error	Error distribution profile
FS-MFCA	Phase	±2%	normal
	Amplitude	±2%	normal
	Frequency	±0.2%	normal
	Beam size	22 μm∼28 μm	uniform
	Offset in two-beam separation	±3 μm	uniform
LR-MFCA	Phase	±4%	normal
	Amplitude	±4%	normal
	Frequency	±0.2%	normal
	Offset in two-beam separation	±3 μm	uniform

In FS-MFCA the amplitude and phase are recorded at 37 different modulation frequencies covering the 10 Hz and 1 MHz range, as shown in Fig. 1 (symbols).

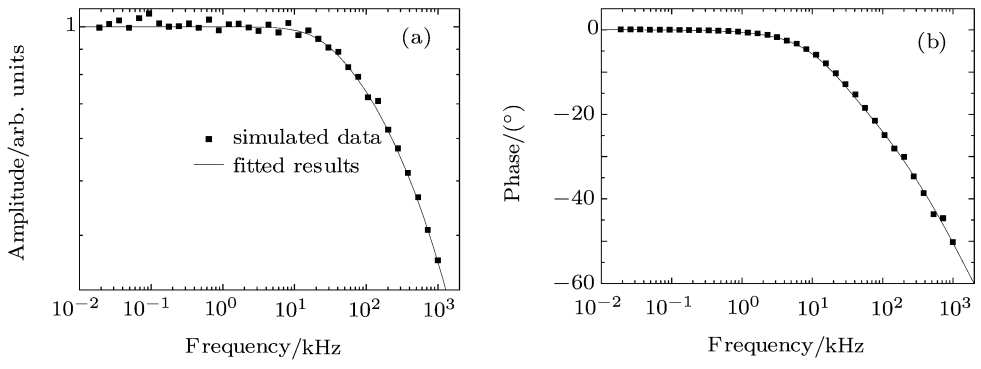


Fig. 1. Simulated FS-MFCA amplitude (a) and phase (b) data and their best fit for a silicon wafer.

For LR-MFCA, a set of amplitude and phase data is created at four different frequencies, as shown in Fig. 2 (symbols). At each frequency, amplitude and phase points are recorded at 15 different two-beam separations. The separation of two spots is chosen to be close to the experimental value, which is determined by the signal-to-noise ratio of the MFCA signal and the sensitivity of the signal-to-individual transport parameter.[18] The simulated amplitude and phase data at all four frequencies are fitted to obtain the three transport parameter values. This simulation and fit procedure is repeated 30 times. Then the fitted results are statistically analysed.

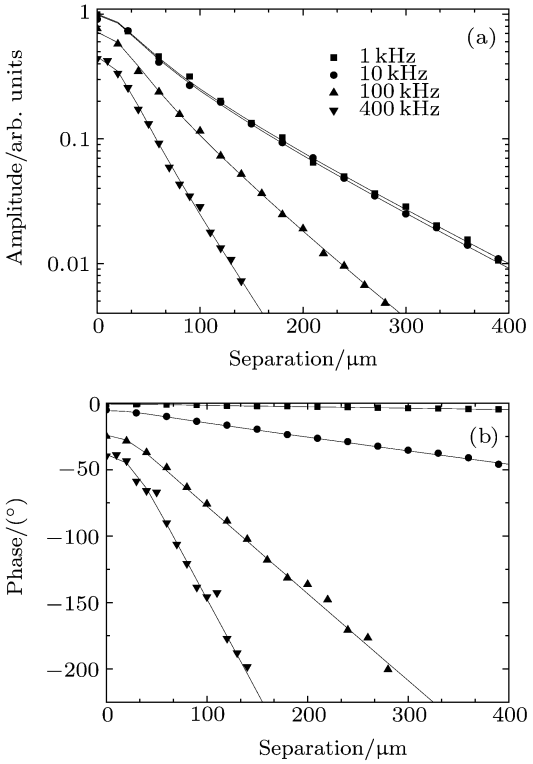


Fig. 2. Simulated LR-MFCA amplitude (a) and phase (b) data and their best fit at frequencies of 1, 10, 100, and 400 kHz, respectively, for silicon wafer.

In the simulations, the following parameter values are used: $D = 20$ cm^2/s, $\tau = 10$ μs, and $S_1 = 10^3$ cm/s. The thickness of the wafer is set to 525 μm. The input parameter values are in typical ranges of the transport properties of high-quality silicon wafers. The fitted results are presented in Table 2 and a typical run of the simulation for FS- and LR-MFCAs is presented in Figs. 1 and 2 (solid lines), respectively. In our case, the selected frequency combination is 1, 10, 100, and 400 kHz in LR-MFCA. We have found from Figs. 1 and 2 that for both FS- and LR-MFCAs, all the simulated data and corresponding theoretical fits clearly agree well for both amplitude and phase. From Table 2, the average amounts of the carrier lifetime, carrier diffusivity and FSRV are 10.4 μs, 20.3 cm^2/s, and 969 cm/s for FS-MFCA; and 10.0 μs, 20.0 cm^2/s, and 1020 cm/s for LR-MFCA, respectively. Apparently, all the statistically mean values of the three fitted parameters are very close or equal to the respective input values. This implies that it is possible to simultaneously determine the lifetime, diffusivity and FSRV by both methods. The mean square errors of the parameters shown in Table 2 is ±2.0 μs, ±2.6 cm^2/s, and ±390 cm/s, corresponding respectively to the percentages of ±22%, ±18%, ±39.3% for FS-MFCA; whereas the mean square errors are ±0.5 μs (±5%), ±0.2 cm^2/s (±1%), and ±167 cm/s (±16.7%) for LS-MFCA. It is evident that the determination accuracies have been improved by a factor of 4.4 for carrier lifetime, of 18 for carrier diffusivity and of 2.4 for FSRV in spite of the higher mean square variance in LR-MFCA than that in FS-MFCA. This reveals that for each parameter, the fitted results of the transport properties determined by LR-MFCA are more reliable than those by FS-MFCA. As was analysed in Ref. [18], this is due to the fact that the sensitivity of the MFCA signal to the individual transport parameter, and especially to the diffusivity, significantly increases with increasing pump-probe-beam separation. Furthermore, we find from Table 2 that in LR-MFCA the statistically mean value of the beam radius is nearly equal to the input values and the corresponding statistical error is only ±0.7 μm (±2.8%). This indicates the feasibility of the simultaneous determination of the beam radius by LR-MFCA. This is particularly important because it is difficult to measure the size of the pump and probe beams. Using the effective radius set as an unknown parameter during the fitting procedure, the reliability of the measurement can be improved. However, further simulation demonstrates that if the beam's radius is also set as a variable in FS-MFCA, all the fitted results including the fitted radius are unacceptable and thus unreliable. Even if in FS-MFCA there is zero measurement error of the spot radius when one calculates simulated data, the statistically mean values of the lifetime, diffusivity and FSRV are (10.3±2.1) μs, (19.9±1.6) cm^2/s, and (1010±330) cm/s, respectively, during which the radius set as a variable is fitted. Corresponding statistical errors are still higher than those determined by LR-MFCA, which are presented in Table 2. Accordingly, another advantage over FS-MFCA is that the effective radius of the exciting beam can be determined with high precision by LR-MFCA.

Table 2. Statistical simulation results for the FS- and LR-MFCA.

	Parameter	Input value	Fitted results	Mean variance
FS-MFCA	Lifetime/μs	10	10.4±2.0	$4.7\pm1.5\times10^4$
	Diffusivity/(cm^2/s)	20	20.3±2.6	
	FSRV/(cm/s)	1000	969±390	
LR-MFCA	Lifetime/μs	10	10±0.5	$1.9\pm0.3\times10^3$
	Diffusivity/(cm^2/s)	20	20±0.2	
	FSRV/(cm/s)	1000	1020±167	
	Radius/μm	25	25±0.7	

4. Experimental results and discussion

The instrumental configuration used for FS- and LR-MFCA is shown in Fig. 3 and has been described in more detail elsewhere.[17,18] Briefly, the excess carriers are created optically by a periodically intensity-modulated diode laser (785 nm) with an optical energy greater than the band gap energy of the wafers and monitored by another continuous diode laser (1570 nm), having an optical energy below the band gap energy. The two beams were made collinear with a beamsplitter arrangement and overlapped within a 25-μm area of the sample surface, which is determined by LR-MFCA. The intensity change ΔI of the transmitted probe beam due to free carrier absorption to the probe beam is measured by an InGaAs photo-detector and recorded by a lock-in amplifier to provide the amplitude and phase of the MFCA signal. The illuminated spot can be moved on the wafer surface by transversely moving the turning mirror and focusing lens assembly in the pump-beam path. The sample used in the experiments is a [100]-oriented p-type silicon wafer, 8 Ω·cm–12 Ω·cm, implanted with P^+ at energy of 80 keV. The thickness of the wafer is 525 μm. The wafer is implanted at room temperature with a dose of 1×10^{10} cm^{-2}.

In FS-MFCA, the amplitude and phase of the signal are recorded as functions of the modulation frequency at zero pump–probe–beam separation. In LR-MFCA the dependences of the amplitude and phase on the two-beam separation are measured at five modulation frequencies: 3, 10, 30, 100, and 400 kHz, by linearly scanning the excitation spot across the centre of the probe spot. In order to determine the transport

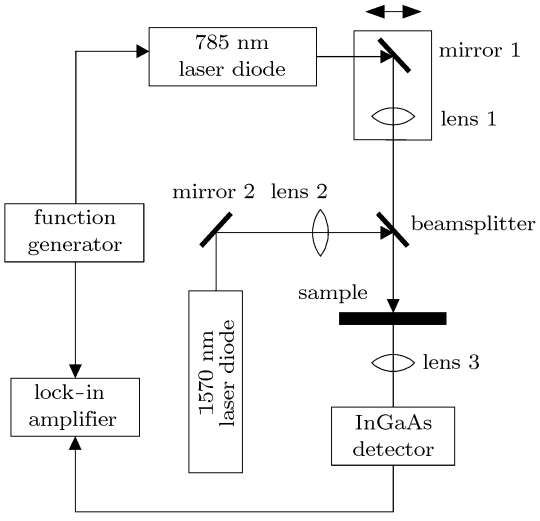


Fig. 3. Schematic diagram of the frequency-scan and laterally resolved MFCA experimental setup.

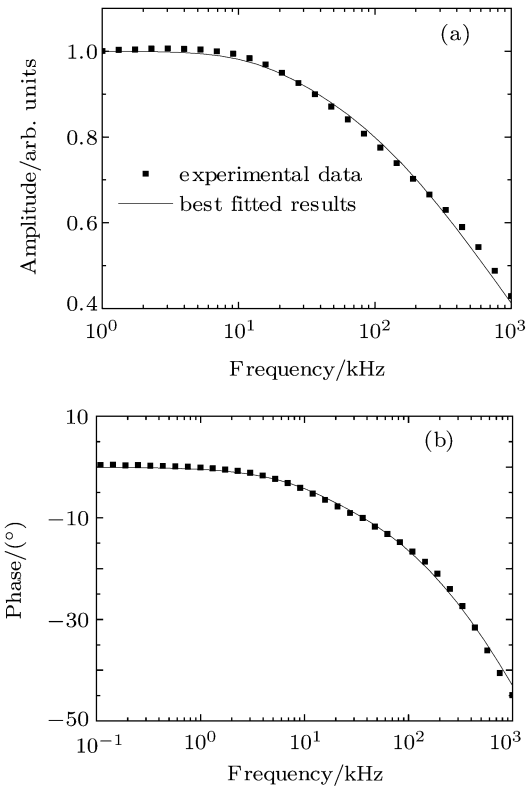


Fig. 4. Dependences of (a) the MFCA amplitude and (b) phase on modulation frequency for a silicon wafer. Symbols: experimental data; solid lines: best-fit curves.

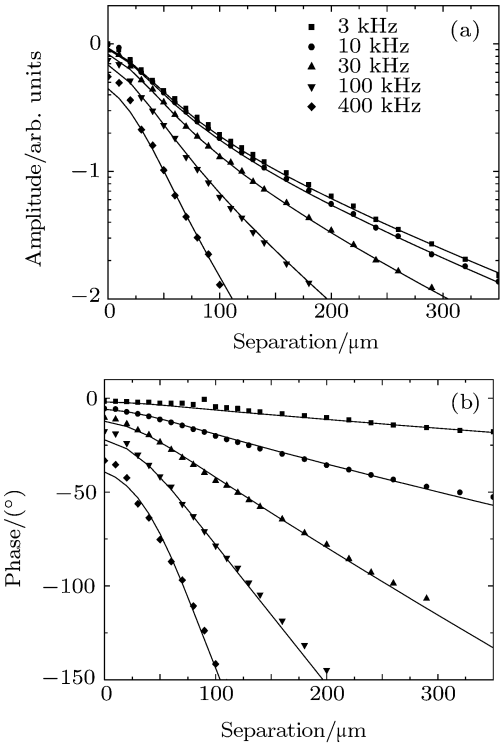


Fig. 5. Dependences of (a) the MFCA amplitude and (b) phase on the pump–probe–beam separation for a silicon wafer, measured at five modulation frequencies: 3, 10, 30, 100 and 400 kHz, respectively. Symbols: experimental data; solid lines: best-fit curves.

parameters of the sample. The experimental data measured in FS- and LR-MFCAs are then fitted to the theoretical model [Eq. (1)], respectively. Figures 4 and 5 present the experimental data (symbols) measured by FS-MFCA and LR-MFCA and the corresponding best fits (solid lines), respectively. The best-fit estimates are $D = 17.6$ cm^2/s, $\tau = 36$ μs, and $s_1 = 16127$ cm/s with a square variance of 7.85×10^{-4} in FS-MFCA and $D = 18$ cm^2/s, $\tau = 33.9$ μs, $s_1 = 11850$ cm/s with a square variance of 1.89×10^{-3} in LR-MFCA. Obviously, for each technique the experimental data and corresponding theoretical fits clearly agree well for both amplitude and phase, as shown in Figs. 4 and 5. Moreover, the differences of the fitted D, τ and s_1 values by FS- and LR-MFCAs are 2.4%, 8.3% and 26%, respectively, indicating that the fitted results using both methods are considerably identical within measurement errors. This implies that both the FS- and LR-MFCA methods can be employed to determine the transport properties of silicon wafers. We have concluded from the analysis in the previous section that the fitted results by LR-MFCA are more accurate than those by FS-MFCA. Furthermore, in FS-MFCA nonlinear recombination,[20,21] the irregularity and uncertainty of the beam radius may render the interpretation of the FS-MFCA experimental results to be very difficult, resulting in the higher uncertainty of the fitted results. On the other hand, in LR-MFCA these factors affect the signal only within the effective radius of the pump beam. Therefore, the determination accuracies of the transport properties by LR-MFCA are more accurate, while there are great measurement errors.

5. Conclusions

A quantitative comparison between FS-MFCA and LR-MFCA from the standpoint of their relative determination accuracies for the transport properties (the lifetime, the diffusivity and FSRV) of the semiconductors by both methods via multi-parameter fitting have been made. By introducing system errors in simulated data, the statistical errors of the fitted results for LR-MFCA are less than those for FS-MFCA. It is justified that compared with FS-MFCA, the LR-MFCA signal is more sensitive to the transport properties and consequently the determination accuracies of fitted results are more reliable. Simulations have also suggested that in FS-MFCA the uncertainty of the size of the pump beam radius can result in an increase in measurement errors of the fitted results, while in LR-MFCA the size of the pump beam radius is a free parameter and can be extracted accurately during the fitting process. In addition, experiments have been performed to determine the transport properties of silicon wafers by FS- and LR-MFCAs, respectively. The fitted results have confirmed that the lifetime, the diffusivity and FSRV could be extracted by FS- and LR-MFCAs, respectively. The experimental results have also indicated that the fitted lifetime, diffusivity and FSRV values obtained by LR-MFCA are more accurate than those by FS-MFCA. The results are in good agreement with the simulated results.

References

[1] Sanii F, Schwartz R J, Pierret R F and Au W M 1989 *Proceedings of the 20th IEEE Photovoltaic Specialists Conference*, 1988 Las Vegas, IEEE, New York p. 575

[2] Sanii F, Giles F P and Schwartz R J 1992 *Solid-State Electronics* **35** 311

[3] Glunz S W and Warta W 1995 *J. Appl. Phys.* **77** 3243

[4] Glunz S W, Sproul A B, Warta W and Wettling W 1994 *J. Appl. Phys.* **75** 1611
[5] Mandelis A, Batista J and Shaughnessy D 2003 *Phys. Rev.* B **67** 205208-1
[6] Batista J, Mandelis A and Shaughnessy D 2003 *Appl. Phys. Lett.* **82** 4077
[7] Li B, Shaughnessy D, Mandelis A, Batista J and Garcia J 2004 *J. Appl. Phys.* 96 186
[8] Li B, Shaughnessy D and Mandelis A 2005 *J. Appl. Phys.* **97** 023701-1
[9] Forget B C, Barbereau I, Fournier D, Tuli S and Battacharyya A B 1996 *Appl. Phys. Lett.* 69 1107
[10] Ikari T, Roger J P and Fournier D 2003 *Rev. Sci. Instrum.* **74** 553
[11] Cheng J and Zhang S 1991 *J. Appl. Phys.* **70** 6999
[12] Mandelis A, Bleiss R and Shimura F 1993 *J. Appl. Phys.* **74** 3431
[13] Salnick A, Mandelis A and Jean C 1996 *Appl. Phys. Lett.* **69** 2522
[14] Shaughnessy D and Mandelis A 2003 *J. Appl. Phys.* **93** 5236
[15] Schönecker A, Eikelboom J A, Burgers A R, Lölgen P, Leguijt C and Sinke W C 1996 *J. Appl. Phys.* **79** 1497
[16] Rodriguez M E, Mandelis A, Pan G, Nicolaides L, Garcia J A and Riopel Y 2000 *J. Electrochem. Soc.* **147** 687
[17] Zhang X, Li B and Gao C 2006 *Appl. Phys. Lett.* **89** 112120-1
[18] Zhang X, Li B and Gao C 2008 *J. Appl. Phys.* **103** 033709-1
[19] Zhang X, Li B and Liu X 2008 *J. Appl. Phys.* **104** 103705-1
[20] Wagner R E and Mandelis A 1996 *Semicond. Sci. Technol.* **11** 289
[21] Wagner R E and Mandelis A 1996 *Semicond. Sci. Technol.* **11** 300